

Application of new methods to evaluate crack closure in the near-threshold fatigue crack growth regime

David Fersini, Alessandro Pirondi*

Dept. of Industrial Engineering, Univ. of Parma, Parco Area delle Scienze, 181/A, 43100 Parma, Italy

Abstract

According to a damage-tolerant approach, fatigue life becomes virtually infinite if the ΔK due to service loads is lower than the threshold for fatigue crack growth (FCG). For this motivation, a proper evaluation of ΔK_{th} is very important. On the other hand, for a given material this parameter appears to be strongly influenced by material microstructure and $R=K_{min}/K_{max}$ ratio. At high propagation velocity this influence is explained by classical closure concept introduced by Elber, but this approach does not always work at threshold. Recently, new methods to account for microstructure and R-ratio effects at low propagation rates were proposed. The aim of this work is to evaluate the effectiveness of those methods testing very different materials: (i) a case hardened steel and (ii) an aluminium matrix particulate composite.

Introduction.

In 1968 Elber discussed some of his observations indicating that crack closure due to interference of opposing surfaces may occur even during the tensile part of load cycles. This observation led to the definition of a new driving force for crack growth that would account for an opening load higher than the minimum load of the cycle:

$$\Delta K_{eff} = K_{max} - K_{open} \quad (1)$$

The underlying assumption is a rigid contact between crack surfaces and, therefore, for $K < K_{open}$ the crack tip is fully shielded. From the experimental point of view, K_{open} is determined from the deviation in the linearity of a load vs. opening curve (see ASTM E-647 regulation).

The anticipated contact of the crack surfaces is mainly related to the residual plastic deformation (PICC) in the steady-state (Paris) FCG regime, while at threshold closure is favoured by microstructural asperities of the fracture surfaces (RICC) or by oxide layers (OICC) that may develop on the fracture surfaces. Anyway, the occurrence of closure due to such mechanisms leads to some criticism about the assumption of a rigid, complete contact of crack surfaces [1]:

- The fatigue crack surface may not interfere at the very tip, but only at some distance behind that.
- PICC can be hardly invoked under plane strain condition, because plasticity is more limited than under plane stress and therefore there is little material sticking off of the crack surface.
- Crack closure due to crack face interference can occur by asperities, oxide layers, etc. but such contributions to crack tip stresses are normally small and are important only in threshold region.

If one considers instead a compliant crack wake [1], the load transfer between crack faces is progressive and therefore there is a local strain contribution even below K_{open} . This means that the value of K_{open} and in turn of ΔK_{eff} cannot simply be determined from the deviation from linearity of the load displacement-curve.

The aim of this work is to evaluate the effectiveness of two alternative methods to evaluate ΔK_{eff} , based on adjusted compliance [1] and partial crack closure (PCC) [2]. These methods were applied to FCG data of very different materials: (i) a case hardened steel and (ii) an aluminium matrix particulate composite. A comparison with the results of Eqn. (1) is then performed.

The ACR and PCC ($2/\pi$) models

The ACR model is based on the hypothesis of a crack driving force proportional to the strain magnitude. A correction to the applied ΔK is made on the basis of the ratio of the measured strain range to ideally closure-free one (Fig. 1). The ΔK_{eff} is then obtained as

* corresponding author, e-mail: pirondia@me.unipr.it

$$\Delta K_{\text{eff}} = \Delta K^* \text{ACR} \quad (2)$$

$$\text{ACR} = (C_s - C_i) / (C_o - C_i) \quad (2\text{bis})$$

where C_i is the specimen compliance before crack initiation, and C_s e C_o are obtained from the load vs. displacement plot for a cracked specimen, see Fig. 1. The ACR parameter is independent from the measurement location. K_{open} is then obtained as

$$K_{\text{open}} = K_{\text{max}} - \Delta K_{\text{eff}} \quad (3)$$

At very low FCG rates, it is known that the more important closure mechanisms are RICC and OICC, which may cause contact not immediately at the crack tip but someway behind that, Fig. 2a. According to this, a PCC model was proposed in [2] that corresponds to the presence of a layer of thickness $2h$ inserted between crack faces at a distance $> d$ from the crack tip

The evaluation of the crack driving force for this situation leads to:

$$K_{\text{max}} - (2/\pi) * K_{\text{open}} - (1 - 2/\pi) * K_{\text{min}} < \Delta K_{\text{eff}} < K_{\text{max}} - (2/\pi) * K_{\text{open}} \quad (4)$$

It can be noticed that ΔK_{eff} is independent from h and for low R-ratios $\Delta K_{\text{eff}} \cong K_{\text{max}} - (2/\pi) * K_{\text{open}}$.

The two models, even though quite different in the formulation, rely on the same physical assumption, that is the crack does not always close completely.

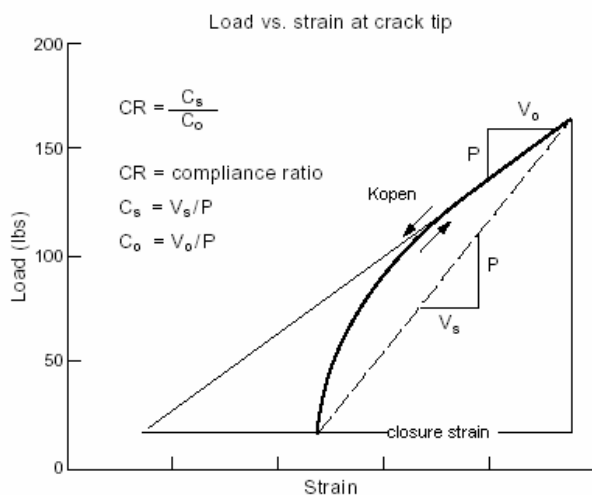


Fig. 1. Comparison between ASTM E-647 offset method for closure level determination, and ACR method for estimating ΔK_{eff} [1].

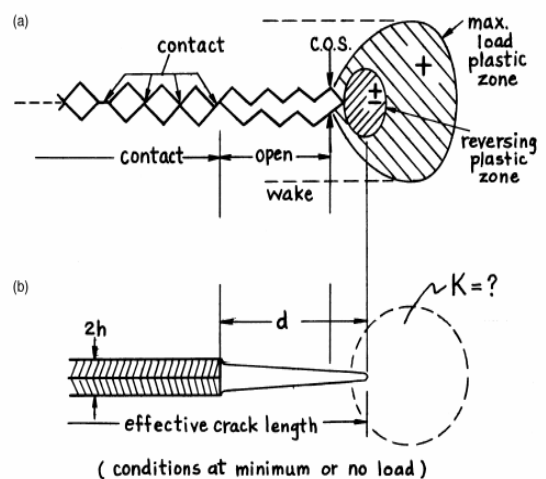


Fig. 2. a) Model of the partial crack closure mechanism; b) parameter definition, [2].

Experiments

Two different materials have been tested: a case hardening steel (i.e. UNI 16 NiCr4Pb) and an aluminium alloy-alumina particulate composite (6061-T6 with 20% vol. of Al_2O_3 particles).

The steel was machined in form of standard RCT specimens (Fig. 3). some of them were quenched and tempered while others were case hardened in a gaseous environment. Small ($24 \times 24 \times 7 \text{mm}^3$) CT specimens of particulate metal-matrix composite (PMMC) were cut in the TL direction from $100 \times 7 \times 1000 \text{mm}^3$ rolled plates (Fig. 4). FCG tests were carried out at a frequency of 10 Hz on a servo-hydraulic testing machine. R-ratios of 0.1 and 0.4-0.5 were used. Specimen compliance was monitored with the back face strain gage technique. The results are reported in Figs. 5 and 6 for steel and CMM, respectively.

Results and discussion

Crack propagation features

The crack path at the specimen side and/or the fracture surface have been observed at the scanning electron microscope (SEM) after testing. To observe fracture surface, the specimens were fatigued at constant load amplitude up to separation. Regarding the PMMC, the RICC is confirmed to be a fundamental mechanism, as shown in Figs. 7 and 8. The fracture surfaces of case hardened steel

(Fig. 9) show plastically deformed regions that can be attributed to contacts between asperities. This let to think to RICC as an important mechanism also in this case. The dark area on fracture surface in Fig. 10 is attributed to the formation of an oxide layer. One can see also a difference in crack growth rate between the center and the sides of the specimen due to the case hardening.

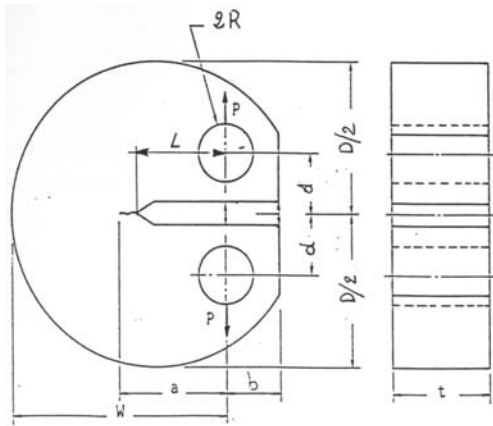


Fig 3. Steel RCT specimen: $t=10\text{mm}$, $W=35\text{mm}$, $L=12\text{mm}$.

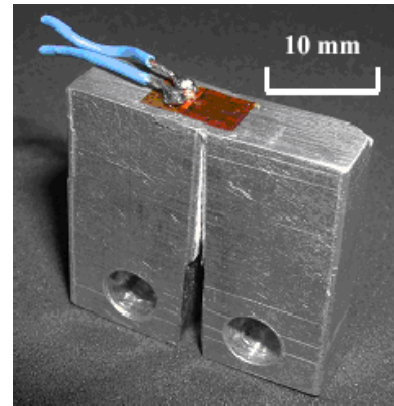


Fig. 4. PMMC CT specimen.

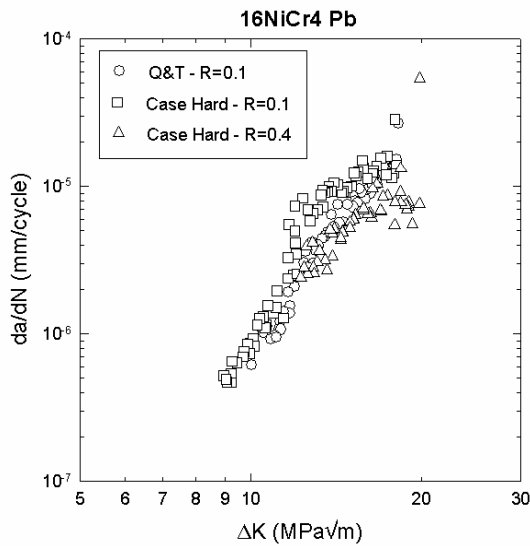


Fig. 5. Experimental data of steel.

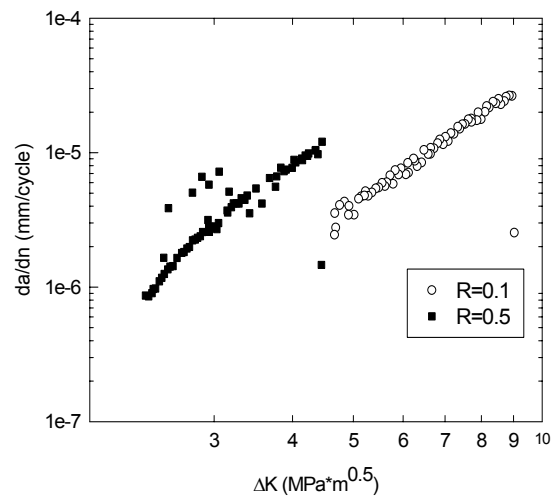


Fig. 6. Experimental data of PMMC.

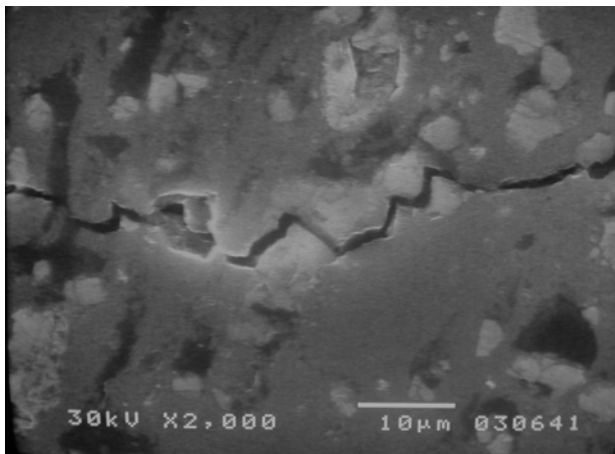


Fig. 7. Sem picture of propagation in PMMC in the near-threshold regime.

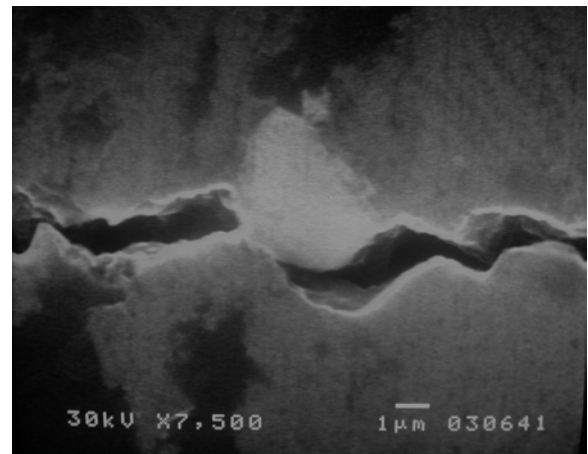


Fig 8. Crack face interaction due to a particle of alumina.

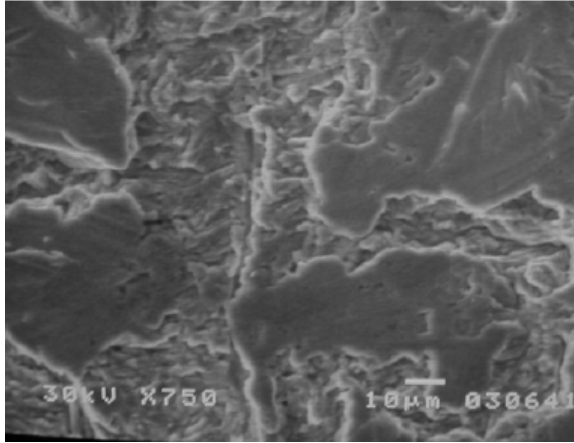


Fig.9. Near-threshold propagation in the hearth of a case hardened steel specimen.



Fig 10. Fracture surface of the case hardened steel tested in the near-threshold region.

Evolution of K_{open} and type of closure

The results are presented and discussed first in terms of K_{open} vs K_{max} . Examples of the evolutions obtained experimentally are reported in Fig. 11 for the case hardened steel tested at $R=0.4$ and in Fig. 12 for the PMMC tested at $R=0.1$, respectively. A linear trend is observed in Fig. 11 with a gradual deviation from linearity towards a constant value for decreasing K_{max} . In the linear portion the K_{open}/K_{max} ratio is in the range $0.3\div 0.4$ for all test conditions. This range agrees with the prediction of the geometrical model of roughness induced crack closure (RICC) proposed by Suresh and Ritchie, [4]:

$$K_{open}/K_{max} = (\tan\theta \cdot \chi / (1 + \tan\theta \cdot \chi))^{0.5} \quad (5)$$

where θ is the deflection angle of the crack path and χ is the ratio between the mode II and mode I displacements at the crack tip. Average values for both θ (i.e. 20°) and χ (i.e. 0.3) were assumed in the present calculations, based on finite element simulations of crack surface roughness [4,5]. The RICC mechanism can be therefore associated with the linear portion of the K_{open} vs. K_{max} relationship shown Fig. 11.

Approaching the threshold condition, K_{max} decreases along with FCG rates. The consequent long testing times promote the generation of an oxide layer. The presence of an oxide layer is confirmed by optical inspection of the fracture surfaces where a darkened area in the vicinity of the crack tip is found (see figure 10). The oxide-induced crack closure (OICC) mechanism adds its contribution to the crack closure behavior causing a deviation from linearity, see Fig.11.

A model correlating the oxide layer thickness, its extension from the crack tip and the level of closure was proposed in [4] and it is summarized by the following equation

$$K_{open} = hE/(1-\nu)(2\pi d)^{0.5} \quad (6)$$

Where E and ν are the Young's modulus and Poisson's ratio of the material and h and d are defined in Fig. 2. When typical values such as $h = 0.1 \mu\text{m}$ and $d = 0.4 \mu\text{m}$ are assumed, [5], $K_{open} = 2.3 \text{ MPa}\cdot\text{m}^{0.5}$. This OICC K_{open} value is very close to the difference between the $K_{open-RICC}$ (obtained by linear extrapolation to the value of K_{max} at threshold in Fig. 11 and the experimental (total) K_{open} at threshold. This result was confirmed in all of the tests performed on case hardened steel. It is worth to remark that the thickness of RCT specimens was such to ensure plane strain conditions, therefore PICC contribution is small.

In the case of the PMMC (Fig. 12) a nonlinear trend precedes the linear part which is, in turn, followed by the gradual shift towards a constant value found also in Fig. 11. The nonlinear part is attributed to PICC since these test was started in the Paris regime (see Fig. 6), where plasticity contribution is important. Approaching stage I, the linear trend is attributed to RICC while the corresponding crack tip opening displacement ($\approx 3 \mu\text{m}$) is similar to the average particle dimension. Since the new surfaces formed by crack advance in the aluminium alloy matrix are prone to corrosion, also OICC becomes evident at low values of K_{max} (Fig. 8).

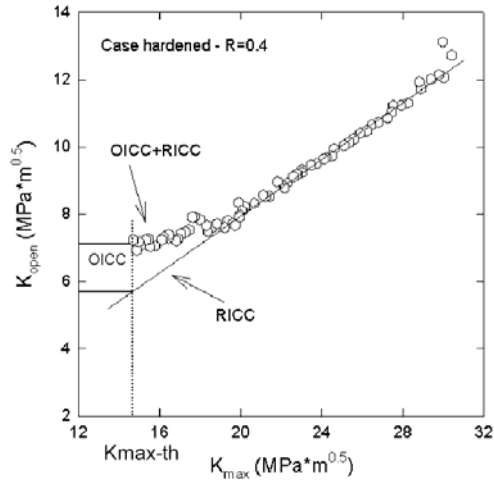


Fig. 11. K_{open} vs K_{max} for a case hardened steel tested at $R=0.4$.

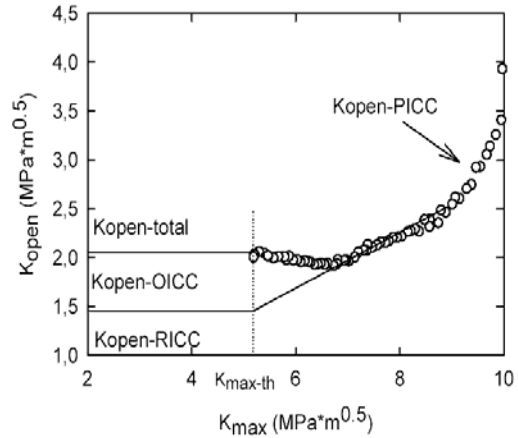


Fig.12. K_{open} vs K_{max} for a PMMC tested at $R=0.1$.

Comparison of different closure models

The value of K_{open} was determined from the deviation from linearity according to the ASTM E647 procedure. Using Eqn. (1) to plot da/dN vs. ΔK_{eff} , the values of the case hardened steel at different R -ratios overlaps well in the steady-state (Paris) regime of FCG (Fig. 13). In the near-threshold regime the situation may even revert, that is higher the R -ratio the lower the crack propagation velocity, as shown in (Fig. 14) in the case of the PMMC.

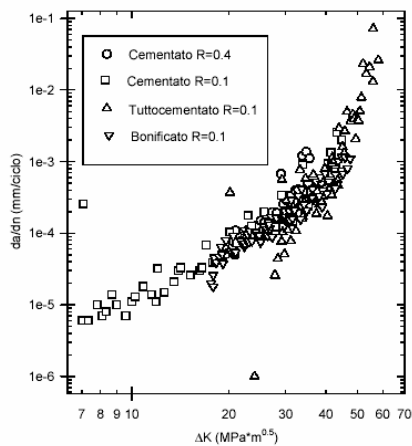


Fig 13. da/dN vs. ΔK_{eff} data in Paris regime for case hardened steel (Eqn. (1)).

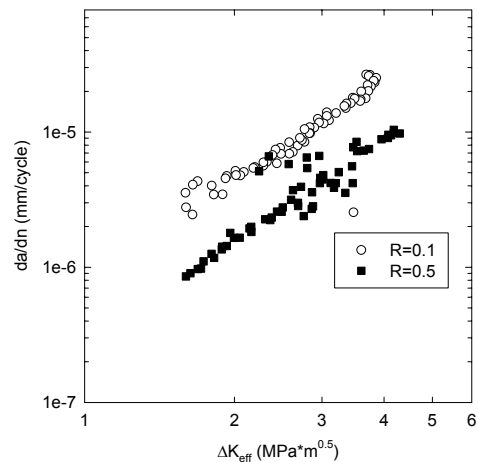


Fig 14. da/dN vs. ΔK_{eff} data in the near-threshold regime for the PMMC (Eqn. (1)).

A case hardened steel specimen was tested also maintaining a constant value for K_{max} , and calculating ACR vs R behavior. The results reported in Fig. 15 demonstrate that the lower the R -ratio the lower the ACR, meaning that at low R -ratios closure is very important, while ACR is unity for R -ratios higher than 0.6.

The experimental data elaborated using PCC model and ACR method showed similar results and a good overlapping of data of different R -ratios for both the case hardened steel and the PMMC. An example of the results is shown for this latter in Fig. 16. The incomplete overlapping of the data is attributed to the brittleness of this material, for which closure cannot explain completely R -ratio effect. In fact, for brittle material also the K_{max} value can play a role in damaging processes.

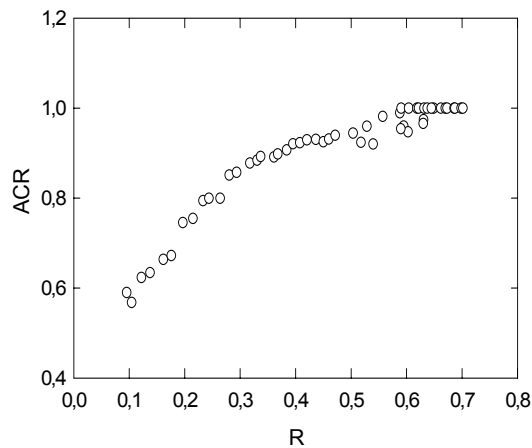


Fig 15. ACR versus R during a constant K_{max} test in the case hardened steel.

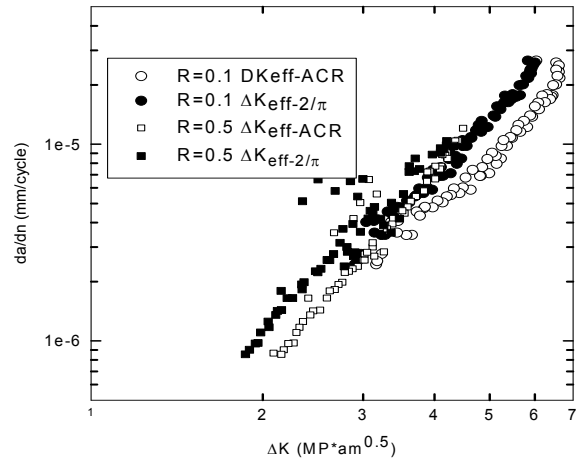


Fig. 16. da/dN vs. ΔK_{eff} data in the near-threshold regime for PMMC (Eqn. (4)).

Conclusions

Two different materials have been tested in threshold region for determining the effectiveness of different method for determining closure and the importance of microstructure in anticipated contact between fracture surfaces. The trend of K_{open} versus K_{max} has been explained in terms of RICC and OICC. The Elber method for determining K_{open} and ΔK_{eff} is effective in Paris region but not in stage I fatigue crack growth. In this regime, the ACR and $2/\pi$ methods give better results than the Elber method.

References

1. J. Keith Donald, "Introducing the compliance ratio concept for determining effective stress intensity" Int. J. Fatigue Vol. 19, Supp. No. 1, S191–S195, 1997.
2. P. C. Paris, H. Tada, J. K. Donald, "Service load fatigue damage - a historical perspective" International Journal of fatigue 21 (1999), S35-S46.
3. D. Fersini, "Near-threshold fatigue crack propagation", Mech. Eng. Thesis, Università di Parma, Italy, 2003 (in Italian).
4. S. Suresh, "Fatigue of materials", Cambridge University Press (1998).
5. D. Fersini, "Evaluation of near threshold fatigue crack growth using of an aluminium alloy-Alumina particulate composites", Imeko 2004, Bologna, Italy.
6. L. Lawson, E.Y. Chen, M. Meshii, "Near-threshold fatigue: a review", International Journal of Fatigue 21 (1999), S15–S34.